

DOE/ER/82744-1

SEPARATION OF METAL IONS FROM LIQUID WASTE STREAMS

FINAL REPORT

DOE Contract No: DE-FG02-99ER82744

Period of Performance:
September 4, 1999 – April 30, 2004

AUTHORS;
D. Gerald Glasgow
Elliot B. Kennel
Applied Sciences, Inc.

John W. Zondlo
Shannon Stover
Y. Xu
West Virginia University

DOE Patent Clearance Granted


Daniel D. Park..

(630) 252-2308
E-mail: daniel.park@ch.doe.gov
Office of Intellectual Property Law
DOE Chicago Operations Office

3/18/05
Date

DISCLAIMER

This report was prepared as an account of work sponsored by an agency of the United States Government. Neither the United States Government nor any agency Thereof, nor any of their employees, makes any warranty, express or implied, or assumes any legal liability or responsibility for the accuracy, completeness, or usefulness of any information, apparatus, product, or process disclosed, or represents that its use would not infringe privately owned rights. Reference herein to any specific commercial product, process, or service by trade name, trademark, manufacturer, or otherwise does not necessarily constitute or imply its endorsement, recommendation, or favoring by the United States Government or any agency thereof. The views and opinions of authors expressed herein do not necessarily state or reflect those of the United States Government or any agency thereof.

DISCLAIMER

Portions of this document may be illegible in electronic image products. Images are produced from the best available original document.

Table of Contents

List of Illustrations.....	3
List of Tables	4
I. Executive Summary.....	5
II. Introduction	6
2.1 Overview of Previous Work	6
2.2 Background Uranium Chemistry	7
III. Experimental Apparatus and Methods.....	10
IV. Results and Discussion	17
4.1 Nanofiber Performance Study.....	17
4.2 Comparison Study	
4.3 Regeneration Study	24
4.4 Identification of Uranium Solids by X-Ray Diffraction.....	25
4.5 Proposed Mechanism	
4.6 Larger Cell Trials.....	27
V. Conclusions and Recommendations	31
VI. References.....	33

List of Illustrations

Figure 1. Equilibrium Concentration of Uranium (IV), from Xu.....	7
Figure 2. Equilibrium Concentration of Uranium (VI), from Xu.....	8
Figure 3. pH/Potential relationship for Uranium Species.....	10
Figure 4. Schematic of Electrolytic Cell.....	12
Figure 5. Experimental Setup Showing Potentiostat, Voltmeter, Peristaltic Pump, Cell, Timer, and Solenoid Valves.....	13
Figure 6. Typical Voltammogram from DPV Analysis of U(VI).....	14
Figure 7. Calibration Curve for Concentration Range 0.5 to 5 ppm.....	15
Figure 8. Calibration Curve for Concentration Range 5 to 100 ppm.....	15
Figure 9. Adsorptive capacities for different nanofibers.....	18
Figure 10: Variation of Applied Potential during sorption versus adsorptive capabilities from the present study (all Voltage's are V (dc) vs. Ag/AgCl).....	19
Figure 11. Stover's Applied Potential diagram.....	19
Figure 12. Repetitive adsorption / desorption from 0 to 90 minutes.....	20
Figure 13. Repetitive adsorption and desorption from 0 to 20 minutes.....	20
Figure 14. Cyclic absorption and desorption from 0 to 45 minutes, from Stover.....	21
Figure 15: The effect of pH on the Adsorptive Capabilities of the cell.....	22
Figure 16. Stover's data showing the effect of solution pH on the U sorption performance.....	22
Figure 17. Results of Electrosorption of Uranium Using Nanofiber Paper Electrodes...	23
Figure 18. X-ray diffraction spectrum.....	25
Figure 19. Schematic of Large Electrolytic Cell.....	32

List of Tables

Table 1. Oxidation/ Reduction Potentials of Uranium Species in water.	9
Table 2. Carbon Nanofiber Production Process Descriptions.....	11
Table 3. Nanofiber Properties	11
Table 4. Results of Carbon Loading Based on the Average of two trials.....	18
Table 5. Results of Regeneration	25
Table 6. Performance of 2” diameter cell.....	27
Table 7. Performance of 4” diameter cell.....	30

I. EXECUTIVE SUMMARY

A unique mechanism was verified for removing uranium from continuously flowing aqueous solutions on a carbon nanofiber electrode with a bias voltage of -0.9 volts (dc versus Ag/AgCl). Uranium concentration was reduced from 100 ppm in the inlet feed to below 1 ppm in a single pass. Cell sizes of 1 cm, 2 inch and 4 inch evaluated during this program were all found to electrosorb uranium from an aqueous stream. The 4 inch cell performed well at uranium concentrations of 1000 ppm. Normally, ordinary electrolysis is not an option for removing uranyl ions because the electrodeposition potential is higher than the dissociation voltage of water. Thus, the ability to electrosorb uranium with greater than 99% effectiveness is a surprising result. In addition, the process was found to be reversible, so that the uranium can be released in a highly concentrated form. In addition to verifying the effectiveness of the system on bench top scale, a regeneration protocol was developed, consisting of passing a 0.1 M KNO_3 solution at a pH of 2.0 and an applied potential of +1.0 V (dc versus Ag/AgCl) which resulted in a measured regeneration of 70% of the electrosorbed uranium. Other experiments studied the effect of pH on electrosorption and desorption, establishing a range of pH for both processes. Finally, it was found that, for an inlet solution of 100 ppm, the carbon nanofiber electrodes were able to electrosorb an amount of uranium in excess of 60% of the electrode mass.

II. INTRODUCTION

The purpose of this Phase II program was to investigate the performance capabilities and capacity of Applied Sciences Inc carbon nanofibers when used in an electrochemical treatment process for uranium removal from water. According to prior studies at West Virginia University (WVU), the ASI nanofibers fared consistently better than other carbon fibers or carbon black, as observed by Xu and later by Stover.^{1,2} Additional experiments were designed to reproduce the prior work, and investigate further the adsorption-desorption process for the electrochemical removal of uranium using ASI nanofibers.

Specific goals of this project were to confirm some of Stover's conclusions, to investigate apparent discontinuities in her data, to clarify the carbon regeneration sequence, and determine performance differences in the types of nanofibers. The repeated experiments clarified discontinuities in the data, such as in applied cell potential, pH, and total loading capacity. Next, there was a study on methods of regeneration of the carbon electrode in order to show the reproducibility of the nanofibers. There was also an attempt to use x-ray diffraction to identify some solid forms of uranium compounds produced during regeneration. Finally, in order to find a difference between adsorptive capabilities of each type of nanofiber, long-term tests were done to detect the total loading capacity for a variety of vapor-grown nanofibers.

These results substantiate the effectiveness of the nanofibers for the electrosorption process of uranyl compounds.

2.1 Overview of Previous Work

Xu studied the electrochemical sorption of uranium as a possible means of removing uranium from aqueous mixtures. The effects of applied potential, pH, flow rates, selectivity, methods of regeneration, and total electrosorption capacity on the performance of the nanofibers in the electrochemical cell were investigated. Xu's work indicated that uranium could be removed by electrosorption under suitable potentials and that ASI nanofiber showed excellent performance for this removal.

Stover continued with Xu's work by trying to relate nanofiber properties resulting from a variety of manufacturing processes to electrochemical removal efficiencies. Nanofiber performance was evaluated using different types of ASI nanofibers produced by these various processes. In addition, the parameters of applied potential, pH, and flow rate were assessed and adsorption/desorption cycling was studied to find optimum conditions for the electrochemical adsorption process. Stover discovered that each type of carbon nanofiber showed the same removal efficiency over a short time period (i.e. 90 minutes). In addition, the optimum operating conditions for the adsorption of uranium were estimated to include an inlet pH of 3.5, a flow rate of 0.7 ml/min, an applied potential of -0.9 vdc (vs. Ag/AgCl). Excellent carbon regeneration was possible for small amounts of electrosorbed uranium. Finally, Stover reported a total nanofiber loading capacity to be a surprising 5.45 gram of uranium absorbed per gram of carbon.

2.2 Background Uranium Chemistry

Uranium consists of three main isotopes: U^{238} , U^{235} , and U^{234} , with U^{238} being the most abundant. Three stable oxides exist, including dioxide (UO_2), trioxide (UO_3), and mixed oxide (U_3O_8).³

UO_2 is a strong basic molecule that is contained in a dark-brown powder. It is insoluble in most acids except for nitric acid (HNO_3), in which it forms uranyl nitrate, $UO_2(NO_3)_2$. UO_3 is much more reactive, combining with most acids to form uranyl salts. U_3O_8 is produced primarily through a combination of UO_2 and air to form a black or dark green powder that is easily transformed into salts.

Uranium can be present in four ionic states: 3+, 4+, 5+, and 6+. Among these states, 6+ is the most common in nature and is the original form of the uranyl ion UO_2^{2+} , which is the ion used in the present study.⁴ These ions dominate the other uranium species, as shown in Figure 1, at a pH of below 2.5. They also become dominated by composite hydrolyzed ions at pH above 2.5.⁵ Due to the strong effects of pH; uranium will undergo hydrolysis and precipitate at a pH above 4.0 as seen in Figure 2.

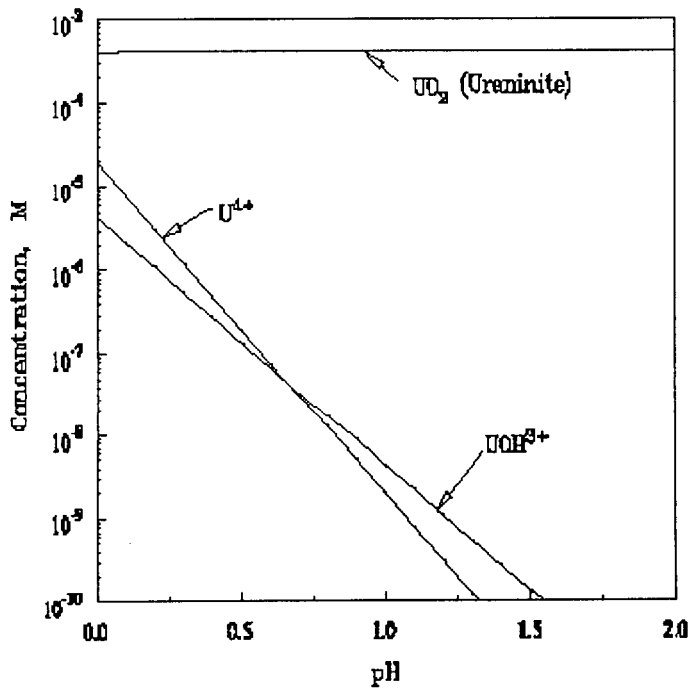


Figure 1. Equilibrium Concentration of Uranium (IV), from Xu.⁶

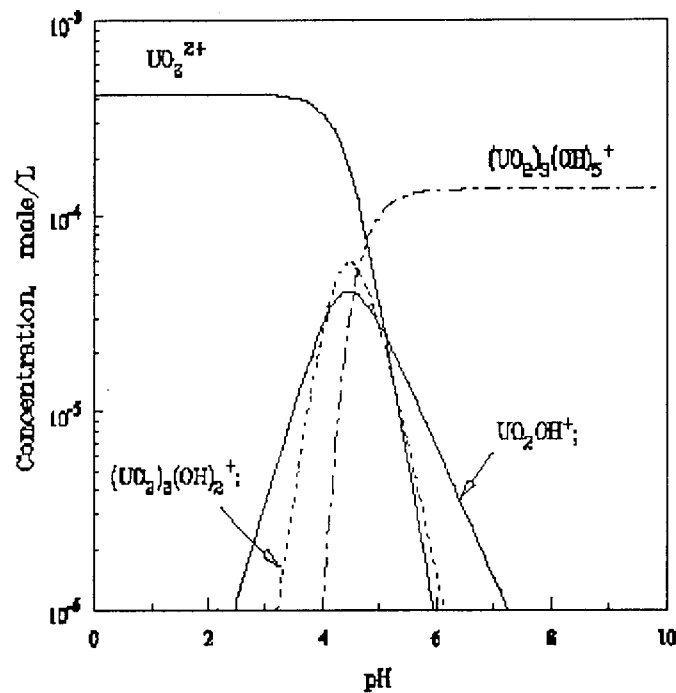


Figure 2. Equilibrium Concentration of Uranium (VI), from Xu.⁷

Another important aspect about uranium is the effect that pH has on electrochemical potential of the uranium-water system. Table 1 and Figure 3 show the electrochemical potentials of the uranyl ion under a variety of conditions.

Table 1. Oxidation/ Reduction Potentials of Uranium Species in water.⁸

Reaction	Potential, V
Two Dissolved Substances	
$U^{3+} = U^{4+} + e^{-}$	$E_0 = -0.607 + 0.0591 \log (U^{3+}/U^{4+})$
$U^{3+} + H_2O = UOH^{3+} + H^{+} + e^{-}$	$E_0 = -0.538 - 0.0591 \text{pH} + 0.0591 \log (UOH^{4+}/U^{3+})$
$U^{3+} + 2H_2O = UO_2^{+} + 4 H^{+} + e^{-}$	$E_0 = 0.612 - 0.2364 \text{pH} + 0.0591 \log (UO_2/UOH^{3+})$
$UOH^{3+} + H_2O = UO_2^{+} + 3 H^{+} + e^{-}$	$E_0 = 0.546 - 0.1773 \text{pH} + 0.0591 \log (UO_2^{+}/U^{3+})$
$U^{3+} + 2 H_2O = UO_2^{2+} + 4 H^{+} + 2 e^{-}$	$E_0 = 0.333 - 0.1182 \text{pH} + 0.0591 \log (UO_2^{2+}/U^{4+})$
$UOH^{3+} + H_2O = UO_2^{2+} + 3 H^{+} + 2 e^{-}$	$E_0 = 0.299 - 0.0886 \text{pH} + 0.0591 \log (UO_2^{2+}/UOH^{3+})$
$UO_2^{+} + UO_2^{2+} = e^{-}$	$E_0 = 0.052 + 0.0591 \log (UO_2^{2+}/UO_2^{+})$
Limits of the Domains of Predominance	
U^{3+} / U^{4+}	$E_0 = -0.607$
U^{3+} / UOH^{3+}	$E_0 = -0.538 - 0.0591 \text{pH}$
U^{4+} / UO_2^{+}	$E_0 = 0.612 - 0.2364 \text{pH}$
UOH^{3+} / UO_2^{+}	$E_0 = 0.546 - 0.1773 \text{pH}$
U^{4+} / UO_2^{2+}	$E_0 = 0.333 - 0.1182 \text{pH}$
UOH^{3+} / UO_2^{2+}	$E_0 = 0.299 - 0.0886 \text{pH}$
UO_2^{+} / UO_2^{2+}	$E_0 = 0.052$
One Dissolved Substance and One Solid Substance	
$U^{4+} + 2 H_2O = UO_2 + 4 H^{+}$	NA
$UOH^{3+} + H_2O = UO_2 + 3 H^{+}$	NA
$UO_2^{2+} + H_2O = UO_3 + 2 H^{+}$	NA
$U^{3+} + 2 H_2O = UO_2 + 4 H^{+} + e^{-}$	a.) $E_0 = -0.382 - 0.2364 \text{pH} - 0.0591 \log (U^{3+})$ b.) $E_0 = -0.019 - 0.2364 \text{pH} - 0.0591 \log (U^{3+})$
$UO_2 = UO_2^{2+} + 2 e^{-}$	$E_0 = 0.221 + 0.0295 \log (UO_2^{2+})$ $E_0 = 0.040 + 0.0591 \log (UO_2^{2+})$
$U_3O_8 + 4 H^{+} = 3 UO_2^{2+} + 2 H_2O + 2 e^{-}$	$E_0 = -0.403 + 0.1182 \text{pH} + 0.0886 \log (UO_2^{2+})$

a. Uranous oxide;

b. Uranous hydroxide, $U(OH)_4$;

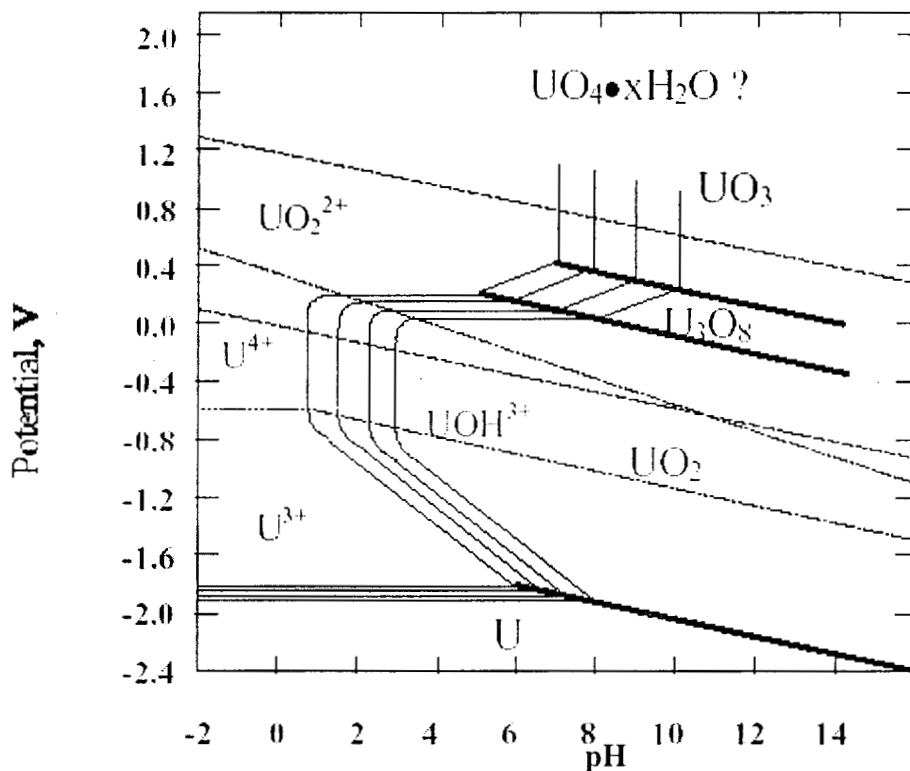


Figure 3. pH/Potential relationship for Uranium Species.⁹

III. EXPERIMENTAL APPARATUS AND METHODS

Carbon nanofibers prepared at Applied Sciences Inc, Cedarville, OH, were used for these experiments. The nanofibers were formed through a catalytic vapor deposition process that allowed for control of nanofiber dimensions such as length and diameter. Typical diameters range from 50 nm to 200 nm with a length of about 100 to 200 microns. In addition, nanofiber surface energy and apparent surface area can be varied by subjecting the nanofibers to different protocols for surface modification and heat treatment.

The nanofibers are labeled to identify the synthesis protocols. The generalized process descriptions are given in Table 2. In addition to the data given in Table 2 there are differences in the gases used for the carbon source. PR-1 and PR-18 used methane whereas the other fiber was based on natural gas as the carbon source. The PR-21 fiber has CO₂ in the reaction gas mixture. The suffix indicates the type of post treatments undertaken, such as Ox400 that indicates air oxidation of the nanofibers in air at 400°C. The PS suffix indicates the nanofiber is pyrolytically stripped in inert gas, an AG suffix that are the as-grown nanofibers with no subsequent treatment, a suffix HT which signifies heat-treatment at 3,000 °C to graphitize the nanofibers. Table 3 lists physical properties of the nanofibers used in this study.

Table 2. Carbon Nanofiber Production Process Descriptions

Nanofiber Designator	Process Description	Relative Reactor Gas Flow Rate	Post Fiber Production Treatment
PR-18 Post Ox	Original fiber production process	1.7X	Air oxidized at 500°C
PR-1 AG	Low production rate process	1X	none
PR-1 ox400	Low production rate process	1X	Air oxidized at 400°C
PR-19 HT	High production rate process using natural gas	4X	3000°C heat treatment
PR-21 PS	PR-19 process using CO ₂	4X	none

Table 3. Nanofiber Properties

	Surface Oxygen (Atomic %)	Surface Area (m ² /g)	Surface Energy (mJ/m ²)	Diameter (nm)	Graph Index (%)	Surface PAH Content (mg/g)
PR-18 post ox	--	--	--	(225)	(55)	0.0
PR-1-ox400	4.6	29	57	(125.0)	(30)	0.0
PR-1-AG	1.1	25	48.0	125.0	31	<1.0
PR-19-HT	0.9	21	275.0	(200.0)	77	0.0
PR-21-PS	1.9	25-35	136.0	(200.0)	(55)	0.0

Values in parentheses estimated based on AG nanofiber values

Various U concentrations were made by dilution of a commercially available 10,000 ppm uranium stock solution adjusted to the desired pH for the experiments. The dilutions were made by mixing the uranium stock solution UO₂(NO₃)₂ at 10,000 part-per million (ppm, mg/l), Plasma Standard, SPEX Industries, Inc., Edison, NJ) with 0.1-M solution of potassium nitrate (KNO₃) and deionized water, which was purified using a NANOpure™ ultra-pure water purification system (Barnstead-Thermolyne, Dubuque, IA). All other chemicals were certified ACS trace metal grade. Unless otherwise noted all solutions were adjusted to a pH of 3.5 (Accumet pH meter, model AR20, Fisher Scientific) by using potassium hydroxide (KOH) and HNO₃ in 0.1-M KNO₃ solution. The small electrolytic cell consists of a laboratory unit with an inside diameter of 1 cm. The volume of the inner cylinder is adjustable so that force could be applied on the carbon bed, thereby reducing air pockets and allowing for better electrical contact and hence a smaller voltage drop across the bed. Even though there was an adjustable cell volume, the total carbon mass remained constant at 0.2 gm neglecting the surface area and density of the nanofibers. In addition, to insure that the void spacing in the nanofiber bed was held relatively constant for the breakthrough experiments, there was an adjustment on the bed volume in order to ensure constant flow rate and minimize oscillations in the peristaltic pump, effectively eliminating the effects of pressure building in the cell.

The cell is equipped with three electrodes. The working electrode is a platinum mesh on which the carbon nanofibers are placed. The reference electrode was a silver/silver chloride (Ag/AgCl) electrode (Bioanalytical Systems Inc., Part No.MF-2021, West

Lafayette, IN). The auxiliary electrode consisted of a bent coil of platinum wire. The oxidation and reduction reactions occur between the working and auxiliary electrodes while the reference electrode establishes a basis for the applied potential. A small distance between all three electrodes is necessary to maintain conductivity and a minimum voltage drop. In addition, a layer of filter paper is placed above and below the carbon nanofibers to prevent them from escaping the cell. Figure 4 is a schematic illustration of the cell and its components.

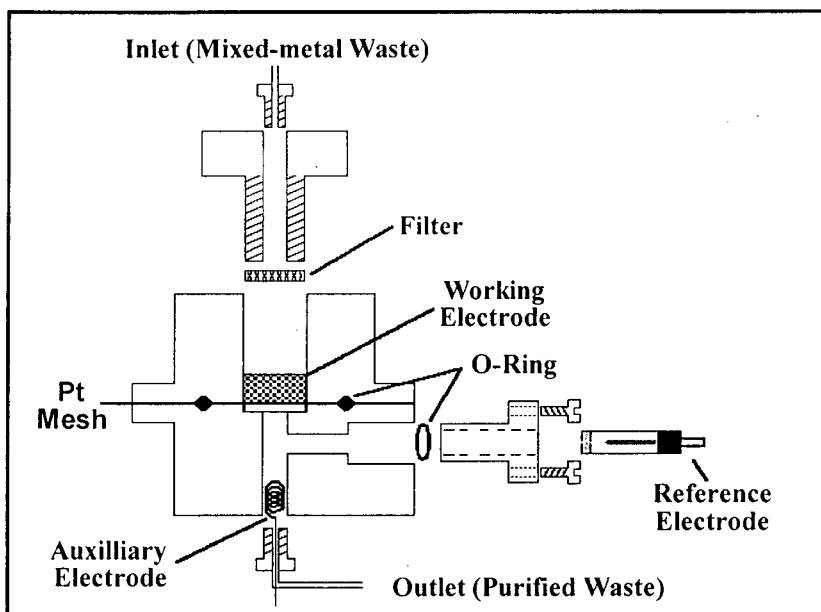


Figure 4. Schematic of Electrolytic Cell.

In the figure, the inlet flow of uranium comes from the top and passes through the carbon, where the uranium is electrosorbed. Next, the flow passes through the platinum mesh where the negative charge is applied versus the reference electrode. The solution finally passes the positively charged auxiliary electrode and exits the cell as purified water.

The direct current potential applied to the carbon nanofibers is generated by means of a potentiostat (Model PWR-3, Bioanalytical Systems, Inc., West Lafayette, IN) that applied a constant voltage (versus the Ag/AgCl reference electrode) to the carbon electrode. The aqueous uranium solution is transported to the cell at specific flow rate by means of a peristaltic pump (Model 7518-60 (driver model 7521-50), Cole Palmer Instrument Company, Vermont Hills, IL). In addition, the applied voltage to the cell relative to the reference electrode is monitored during the experiments by means of a digital voltmeter (Keithley 2700 multimeter/data acquisition system, Integra Series, Keithley Instruments, Inc., Cleveland, OH). Seven solenoid valves (BIO Chem. Valve Inc., P/N 075T2NC12-32) and a programmable timer (Industrial Timer Company, Model RC-10, and Gear A-24) are used for sample collection during unattended operation. Figure 5 shows the actual laboratory setup.

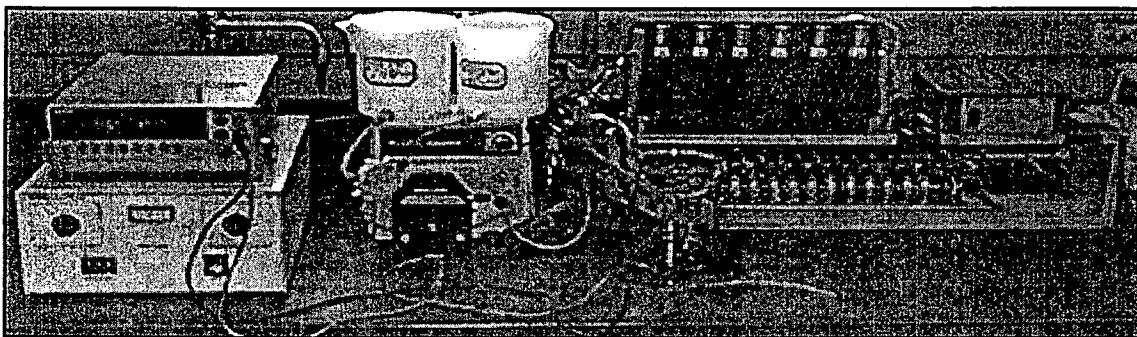


Figure 5. Experimental Setup Showing Potentiostat, Voltmeter, Peristaltic Pump, Cell, Timer, and Solenoid Valves.

0.20 grams of carbon nanofibers were placed firmly into the cell body with a filter paper gasket. The cell was tightened until the nanofibers were snugly packed. Next, the 0.1 M KNO_3 solution at pH of 3.5 was passed through the cell at a potential of +1.00 V (dc) (versus Ag/AgCl) for 30 minutes at a flow rate of 0.7 ml/min. The same solution was then passed through the cell for an additional 30 min at -0.9 V (dc). These two periods are necessary because the production of the nanofibers involves the use of iron (Fe) catalyst and other unidentified materials that interfere with the subsequent analysis of the uranium. Next, the cell was switched to a potential of zero and the flow of the 100-ppm uranyl nitrate solution begun. This was maintained until the effluent concentration equals that of the inlet. Then the cell potential was switched to -0.9 V (dc) and sampling commenced. One sample was taken every 10 min for the first hour, then less frequently thereafter. Due to the low flow rate, each reported data point was an average over the sampling time thus possibly affecting the first data point at 10 minutes due to the initial high concentration of uranium. For all experiments, except where noted, the inlet concentration of uranyl nitrate was held relatively constant at 100 ppm along with the flow rate at 0.7 ml/min and a pH of 3.5.

Additional trials were carried out to clarify the stripping techniques prescribed by Xu. The protocols were carried out in accordance with Stover's protocols, with the exception that the nanofibers were the PR-18-post-oxidized type.

For the analysis of each of the samples, differential pulse voltammetry (DPV) was chosen. This is accomplished by means of a static mercury drop electrode (SMDE) (Model 303A, EG&G Instruments, Princeton Applied Research, Princeton, NJ), a potentiostat/galvanostat (Model 263A, EG&G Instruments, Princeton Applied Research, Princeton, NJ), and electrochemical software (Model 250, EG&G Instruments, Princeton Applied Research, Princeton, NJ). Each sample is collected over a ten-minute period, placed in the mercury drop apparatus, and purged for four minutes with nitrogen to remove excess oxygen from the sample. The test commences with a voltage scan that begins at -0.4 V (dc) and increases to -0.05 V (dc). This reduces the U (VI) to U (V) causing a current peak to appear at approximately -0.17 V (dc, versus Ag/AgCl reference electrode). As previously shown by Pourbaix, the relationship between pH and potential yields the expected reduction potential of U (VI) to U (V) to be +0.052 V (dc). Thus, adding this from a reference electrode of -0.22 V (dc) should achieve a peak at -0.168 V (dc) as shown in Figure 6.

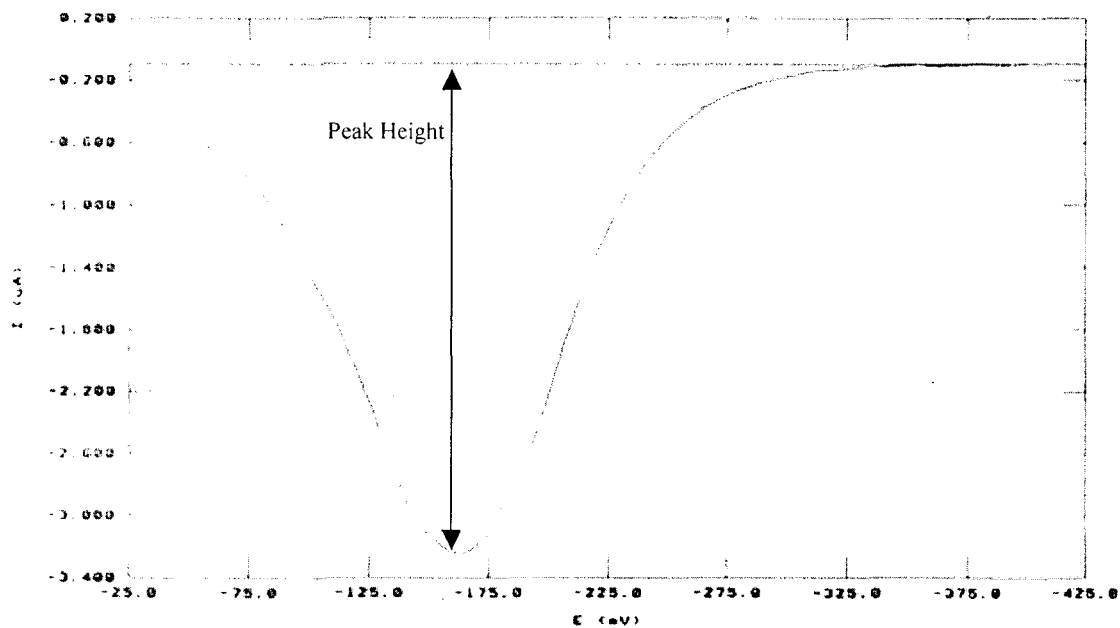


Figure 6. Typical Voltammogram from DPV Analysis of U(VI).

The height of this peak is due to the amount of current that flows during the analysis and is directly proportional to the concentration of U (VI) present in the sample. By using standard solutions of known U concentrations, a calibration curve for the concentration of uranium in the sample solution versus current peak height is developed. In order to acquire a more accurate calibration, there should be separate curves for the high concentration (>5 ppm) and low concentration (< 5 ppm) regions as seen in Figures 7 and 8.

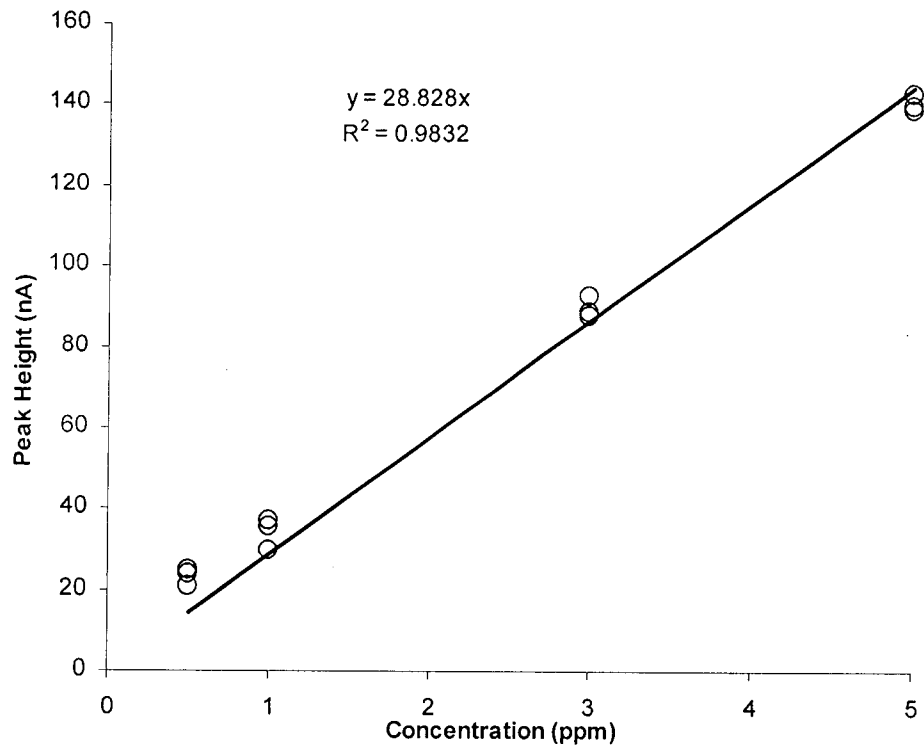


Figure 7. Calibration Curve for Concentration Range 0.5 to 5 ppm

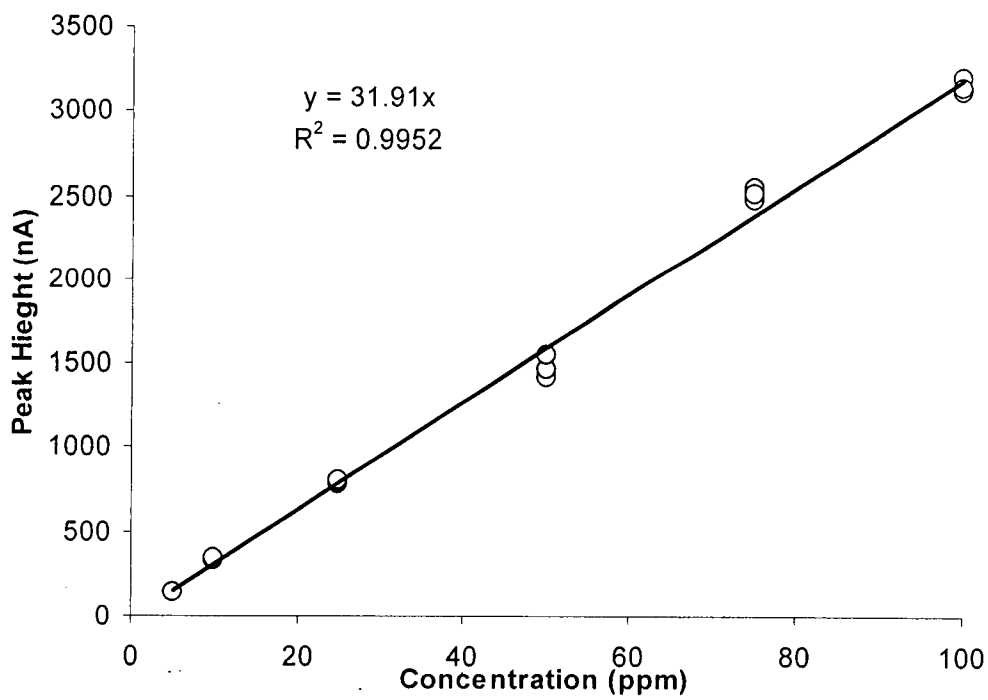


Figure 8. Calibration Curve for Concentration Range 5 to 100 ppm

Following the electrosorption of the uranium, the carbon electrode can be regenerated by applying a potential +1.00 V (dc, versus an Ag/AgCl reference electrode) to the cell and passing a 0.1 M KNO₃ solution at pH 2 for 45 minutes. The reason for such a low pH was that when a higher pH is used, the regeneration of the carbon is not as complete. As discussed below, several regeneration techniques were tested and the one described here was found to be the most effective.

Two larger cells used in this program were also equipped with three electrodes. The working electrode for both these cells was a carbon fiber mesh on which the carbon nanofibers are placed. The reference electrode is a silver/ silver chloride electrode. The auxiliary electrode is a graphite electrode made a high permeability porous graphite (grade PG-25) obtained from Morgan Specialty Graphite. The inlet flow of uranium comes from the top and passes through the carbon, where the uranium is electrosorbed. Next, the flow passes through the carbon fiber mesh where the negative charge is applied versus the reference electrode. The solution finally passes the positively charged auxiliary electrode and exits the cell.

The carbon nanofiber used in these cells was in the form of paper or mat. One paper was formulated from carbon nanofibers, a small percentage of PAN carbon fibers and an unidentified binder. This paper was supplied by an organization who was evaluating carbon nanofibers for a proprietary application and were not willing to identify the binder. The second paper was prepared at ASI as follows. The fiber was combined with 20% (by wt.) uncured natural rubber by mixing the following formulation for 20 min. in a high shear mixer:

- 1 lb PR-24 (as grown)
- 22 gm T-DET (N-9.5) nonionic surfactant from Harcos Chemical
- 200 gm Natural Rubber Latex, low ammonia, 60% natural rubber.
- 6 gal. water

The formulation has been balanced to achieve coagulation of the rubber latex upon the surface of the fiber under high shear mixing as described in Applied Sciences U.S. Patent No. 5,594,060, "Vapor Grown Carbon Fibers with Increased Bulk Density and Method for Making Same."

Making Paper:

Twenty-five gm. of coated fiber were vacuum filtered through Fisher Q2 fine porosity paper. The filtrate was clear. The paper was separated from the fiber mat and dried under weights @ 85°C for 4 hours. The sample was friable, but could bend easily. The Density was 0.13 gm/cc (0.6 gm deposited and 0.05 cm thickness).

The direct current potential applied to the carbon nanofibers is generated by means of a DC power supply (Hewlett Packard 6282A) that applies a constant voltage (versus the Ag/AgCl reference electrode) to the carbon electrode. The aqueous uranium solution is pumped through the cell at specific flow rate by means of a peristaltic pump (Manostat Manufacturing Co., Varistelic Pump, solid state). In addition, the applied voltage to the cell relative to the reference electrode is monitored during the experiments

by means of a digital voltmeter (Keithley 130, Keithley Instruments, Inc., Cleveland, OH).

IV. RESULTS AND DISCUSSION

The performance of various nanofibers for the electrochemical removal of uranium was assessed in these experiments. The mercury drop technique was used for the analysis of several uranium samples supplied to WVU by ASI. The manufactured and treated nanofibers were created by the methods previously mentioned; the properties of the nanofibers were intentionally varied during manufacture using differences in the nanofiber production conditions. Each nanofiber was tested both for uranium removal efficiency and for ultimate uranium capacity. In addition, in order to clarify and reassert some of Stover's data, the effects of adsorption / desorption, pH, and potential were reinvestigated in more detail to find a clear consistency in her data. Finally, a study involving the regeneration sequence of loaded nanofibers was investigated so that parameters for complete regeneration of the nanofibers could be determined.

4.1 Nanofiber Performance Study

Six selected nanofibers were tested to construct observable breakthrough curves and determine nanofiber capacity for uranium sorption. The experimental conditions were tested at an inlet concentration of 100 ppm uranium, a pH of 3.5, and a flow rate of 0.7 ml/min, with 200 mg of the nanofibers in the cell. For all experiments, the concentration started at 100 ppm U and dropped rapidly to around 0 ppm. The experiment would continue until the concentration of the effluent would become greater than zero, indicating the breakthrough time of the carbon. In addition, each experiment was done twice for reproducibility.

Table 4 illustrates the data collected from these experiments. Equation 1 is used to calculate the mass of uranium adsorbed. This quantity is then divided by the mass of carbon m_c (i.e., 200 mg) to obtain the ratio between the mass of uranium absorbed per mass of carbon present in the electrode.

$$m_u = C_u \Delta t \dot{V} \quad (1)$$

where m_u is the mass of uranium in milligrams, C_u is the concentration measured in milligrams per liter, Δt is the duration of the experiments in minutes, and \dot{V} is the flow rate measured in liters per minute.

Table 4. Results of Carbon Loading Based on the Average of Two Trials.

Nanofiber Designator	m_u/m_c	Total adsorbed uranium, g
PR-18 Post Ox	0.523	0.107
PR-1 AG	0.411	0.085
PR-1 ox400	0.359	0.073
PR-19 HT	0.373	0.078
PR-21 PS	0.621	0.127

Clearly, there is an advantage to the adsorptive capacity of PR-21-PS, and PR-18 post ox with a higher m_u/m_c of 0.621 and 0.523 respectively. PR-21-PS and PR-18 post ox have only one similarity in that they are both pyrolytically stripped. The next closest is PR-1 AG with m_u/m_c of 0.411. Figure 9, below shows the breakthrough curves for each type of nanofiber.

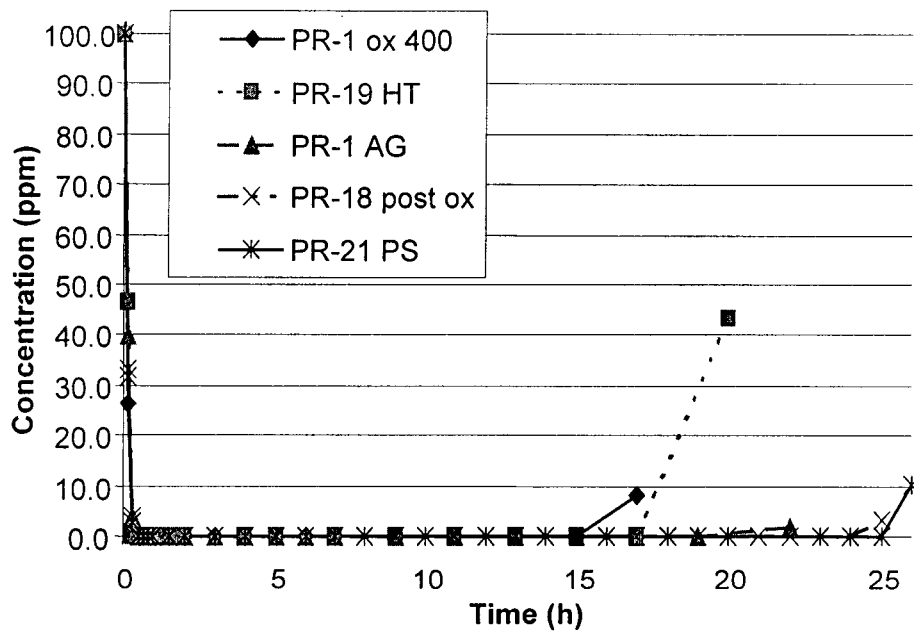


Figure 9. Adsorptive capacities for different nanofibers.

The numbers are significantly different from the findings of Stover. Stover reported an adsorption ratio m_u/m_c equal to 5.45 for PR-1-ox-400, compared to 0.359 in the present study. The former result was achieved using an inlet concentration of 1,000 ppm continuing until the exit concentration rose from nearly zero to 832 ppm. By contrast, the present study used an inlet concentration of 100 ppm. Even so, the large difference between the capacity values cannot be readily explained.

4.2 Comparison Study

There were three other parametric studies done in this project: the first on the effect of changing potential during the sorption of U, the second on the effect of multiple sorptions / desorption cycles, and the last on changing pH. This reinvestigation is for the further clarification of the work done by Stover. The present study has verified that much of the previous work done by Stover is reproducible. For some cases, more detailed testing was performed to clarify the effect of parameters more fully.

Figures 10 and 11 shows a comparison of the data from the present study to that of Stover's earlier work. This comparison is between the variations of cell potentials during sorption of U. The two experiments were set up identically with one exception: PR-18 post ox was used in the most recent study to compare with PR-1 ox 400 that was used in the previous study. Similar results were achieved with both variants. As seen in both these figures, significant U removal occurs between potentials of -0.3 and -0.5 V. Thus, the minimum acceptable potential is shown to be -0.5 V.

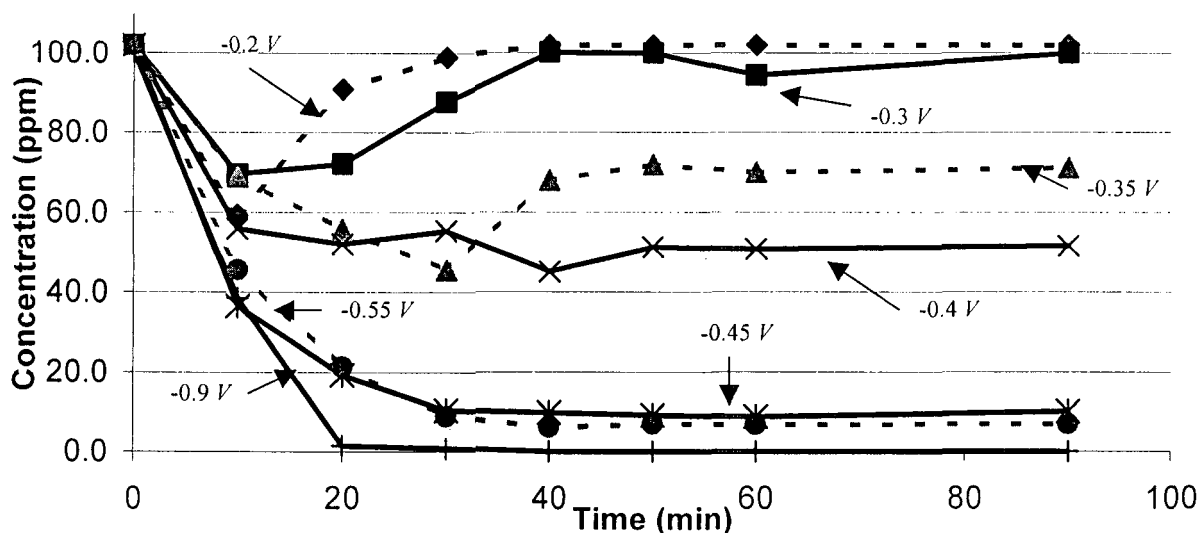


Figure 10: Variation of Applied Potential during sorption versus adsorptive capabilities from the present study (all Voltage's are V (dc) vs. Ag/AgCl)

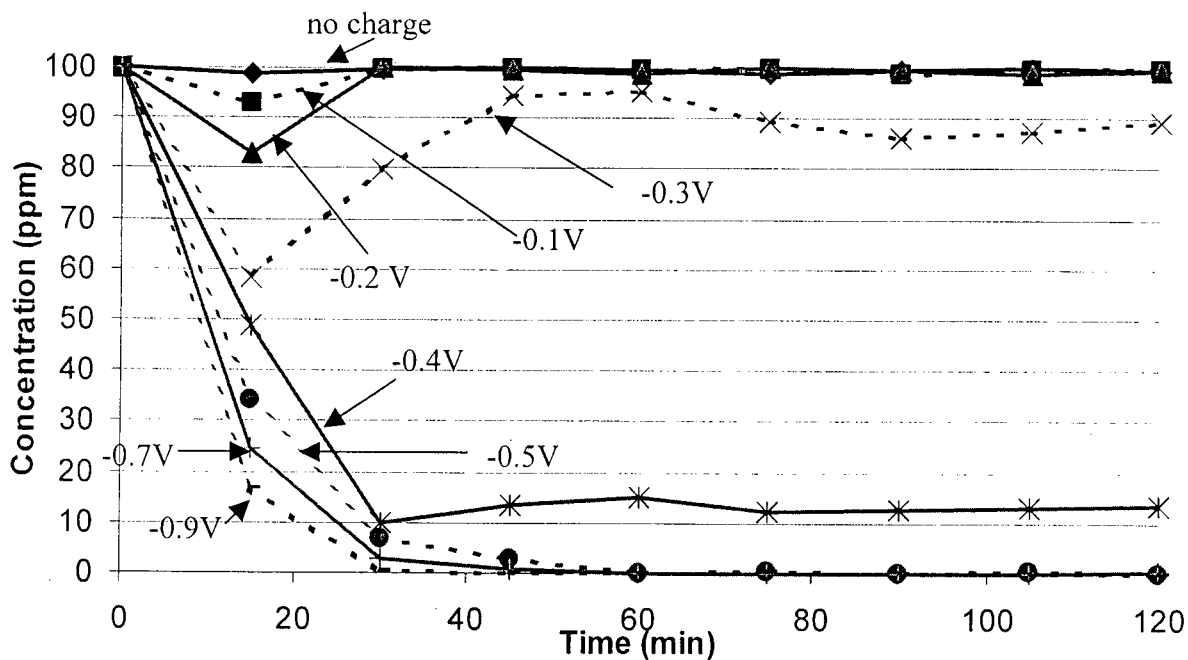


Figure 11. Stover's Applied Potential diagram.¹⁰

Next the study on cycling between adsorption/desorption was performed. Test conditions for these runs were a constant inlet concentration of 130 ppm of U in 0.1 M KNO_3 at a pH of 3.5 with a flow rate of 0.7 ml/min. Each run was 90 minutes and stripping between runs was accomplished with a 0.1 KNO_3 solution at a pH of 2.0 and +1.00 V charge for 45 minutes. Careful attention was paid to cycling the same carbon electrode through many adsorption/ desorption cycles. Figures 12 and 13 demonstrate that effective uranium removal persists over many cycles at least for the relatively short sorption time of 90 min. In addition, Figure 14 shows the distinct similarity between the data collected here and by Stover.

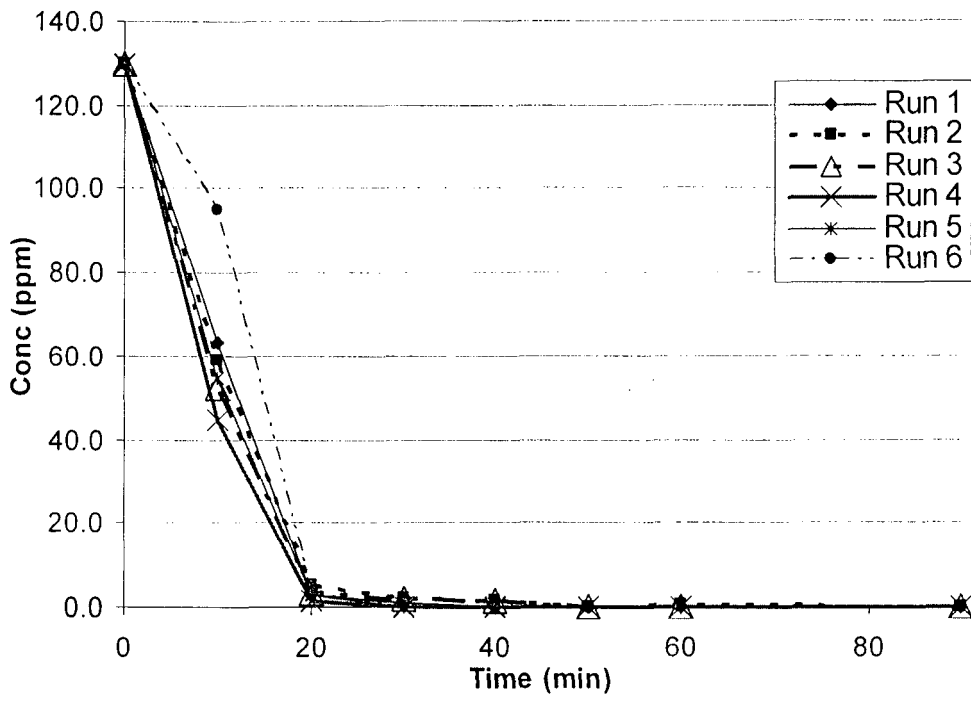


Figure 12. Repetitive adsorption / desorption from 0 to 90 minutes.

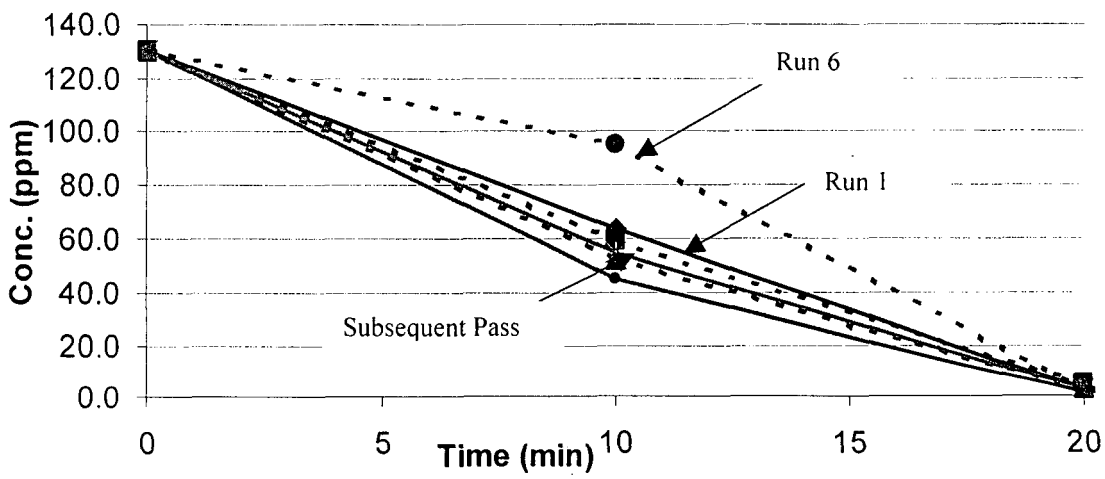


Figure 13. Repetitive adsorption and desorption from 0 to 20 minutes.

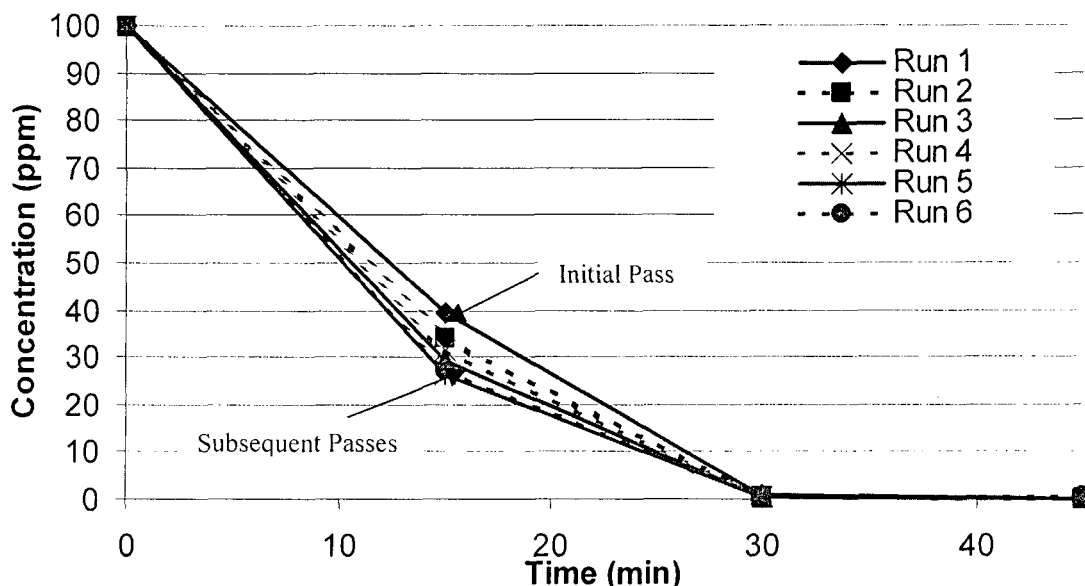


Figure 14. Cyclic adsorption and desorption from 0 to 45 minutes, from Stover.¹¹

The effect on adsorption of pH over the range of 2.0 to 3.5 was observed. The sorption study consisted of an inlet concentration of 100 ppm in 0.1 M KNO_3 solution with a flow rate of 0.7 ml/min and a potential of -0.9 V for 90 minutes, the stripping was done at +1.0 V (dc) with 0.1 M KNO_3 and a pH of 2.0 for 45 minutes. Figure 15 and Figure 16 shows the same sorption behavior for pH of 3.5 and pH of 2.0. Figure 15, shows additional tests at the pH of 2.5 and 3.0 in order to investigate in more detail the effects of pH on the sorption of the uranyl ion. The results in Figure 15 compare favorably with those of Stover's in Figure 16 for pH of 2 and 3.5. Furthermore, Figure 15 demonstrates that a pH of greater than 3 is needed for effective U removal. At lower pH, the uranyl ion is very stable in solution and strongly resists absorption on the carbon electrode. At pH greater than 5.0, the uranyl ion precipitates and hence is not available for removal. The data suggest that the pH should be between 3 and 5 for effective electrosorption.

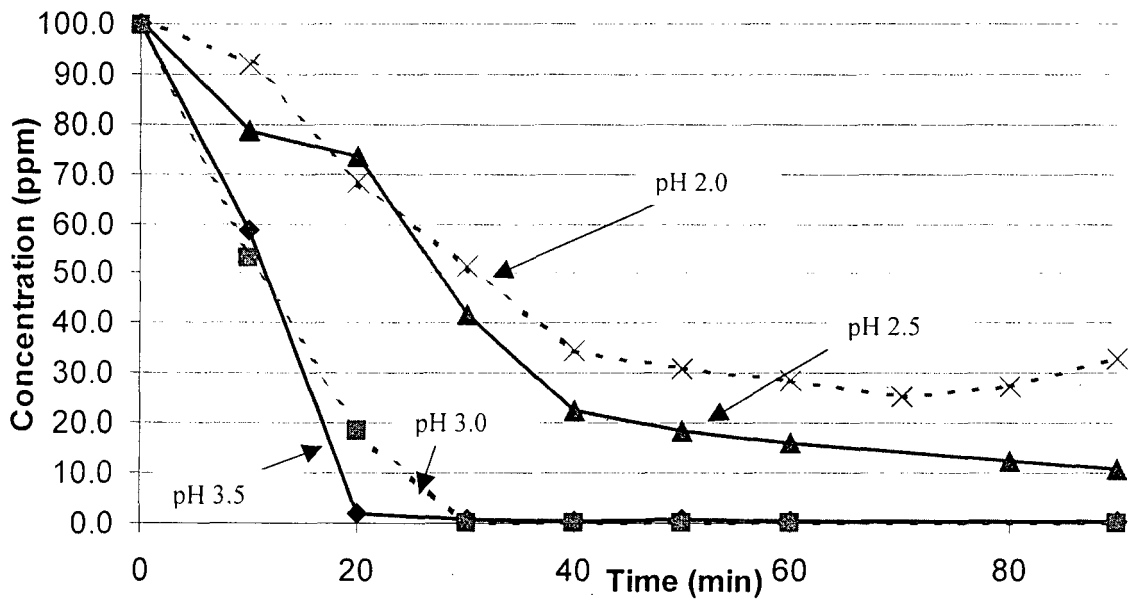


Figure 15: The effect of pH on the Adsorptive Capabilities of the cell.

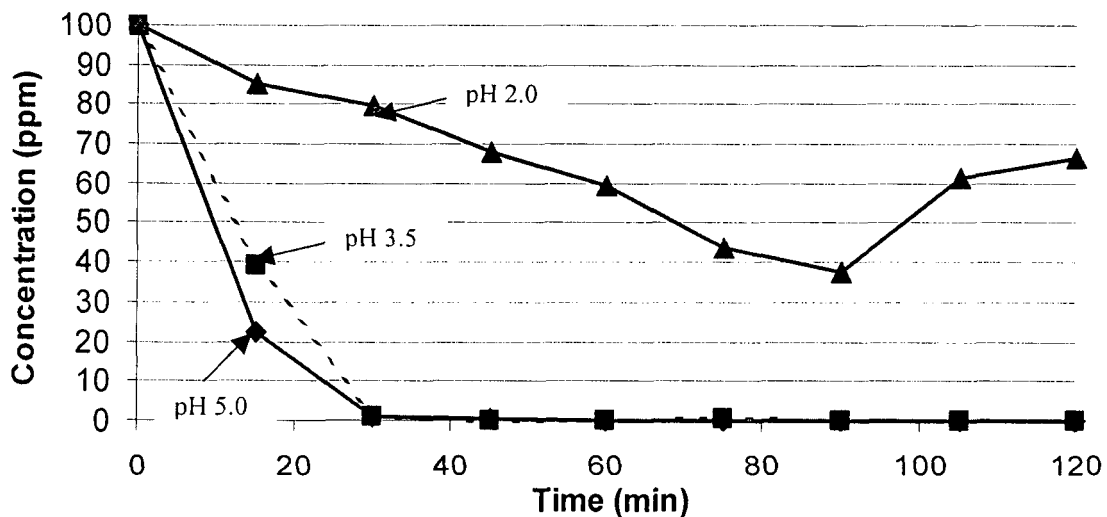


Figure 16. Stover's data showing the effect of solution pH on the U sorption performance.¹²

ASI also supplied WVU with an experimental test paper fabricated from carbon nanofibers. This was placed into the cell shown in Figure 4 and tested under standard electrosorption conditions. However, the carbon nanofiber paper did not work as well as the loose nanofibers in the small cell design. Perhaps this is due to relatively low porosity of the paper. In Figure 17, the results of running the cell with the paper electrode for two consecutive times are shown. The paper did adsorb some uranium but the adsorption was not as great as it was with the previous nanofibers tested over the short time period.

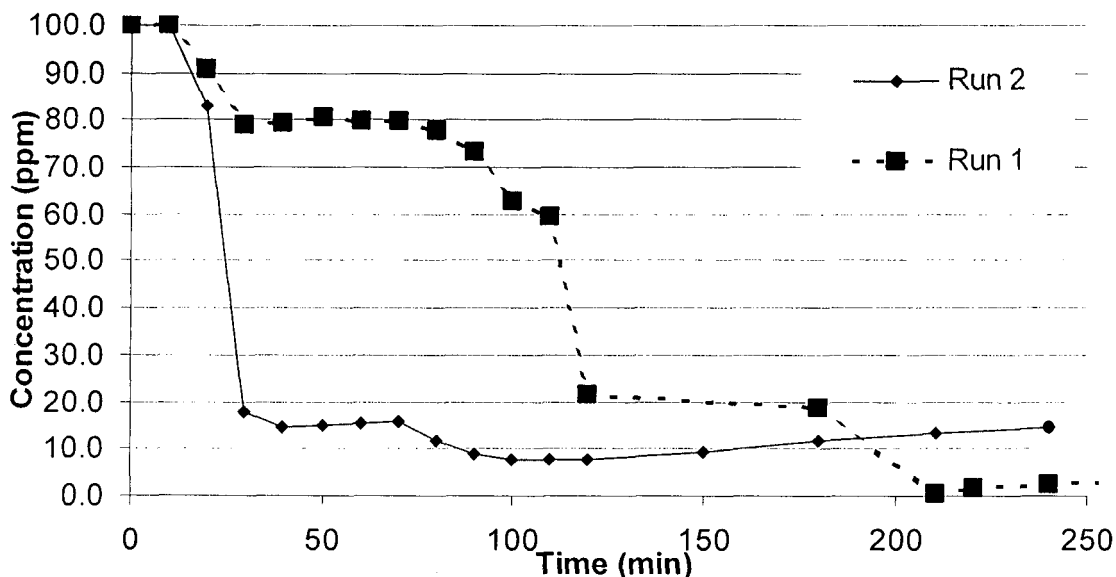


Figure 17. Results of Electrosorption of Uranium Using Nanofiber Paper Electrodes

The poor performance in the first run is probably due to the cell not being tightened enough. Consequently, the paper segments acted as baffles, and the solution could flow around the paper segments rather than through them. Each observed drop in the diagram for run 1 reflects additional tightening of the cell, thus decreasing the volume of the electrode and forcing more fluid to contact the carbon. The second run was operated at the lowest possible cell volume and it looks closer to the expected values for the nanofibers. However, it still is not as good in the cell as the previously tested nanofibers. This suggests that the lack of open porosity influences the results.

4.3 Regeneration Study

The purpose of the regeneration study was to determine the effectiveness of reverse biasing to regenerate the nanofiber electrode. These trials were performed with PR-18-post-ox. This was presumed to be representative of all other carbon nanofibers due to the similarities shown in all previous test runs. For each trial, normal electrosorption was carried out for 90 minutes with a 100 ppm uranium feed at a potential of -0.9 V (dc). Then the inlet solution was changed to 0.1 M solution of KNO_3 at the adjusted pH and a positive potential was applied. The varying factors in the tests on stripping methods were using different pHs and potentials, with these conditions held constant until the concentration of effluent reached 0. Table 5, is a collection of the data acquired through the regeneration study.

Table5. Results of Regeneration

pH	Potential, volts (dc)	Mass of Adsorbed uranium on carbon, mg	Mass of uranium collected from Carbon, mg	Collected uranium fraction, %	Time for Collection (min)
2.0	0.00	7.19	4.88	68	120
2.0	+1.00	7.22	5.06	70	60
3.5	+1.00	8.05	3.55	44	100

With a pH of 3.5 and a potential of +1.0 V (dc), there was only 44 % observed regeneration over a two-hour period, while with a pH of 2.0 at a potential of +1.0 V (dc) there was 70 % observed regeneration over just a 60-minute period. For the pH of 2.0 all the uranium ions come out in solution. However, with a pH of 3.5, about 1% of the net weight of U in the cell leaves as an unknown yellow precipitate while the rest of the U observed leaving the cell comes out in solution. Note that for the case of a pH of 2.0 with no applied potential, it took twice as long to achieve the same removal. Thus, it is clear that for the highest possible regeneration in the shortest time, a low pH, and a positive potential are desirable.

4.4 Identification of Uranium Solids by X-Ray Diffraction

Three different uranium containing solids were obtained by different methods in order to try to better identify the precipitate leaving the cell during regeneration with the pH of 3.5 and potential of +1.00 V. The first solid was generated by collecting the precipitate leaving the cell. The second was made by adding KOH to a solution of 100 ppm U in 0.1 M KNO₃. This mixture precipitates an unidentified uranium compound when the pH is above 5.00. The third and final solid was formed by evaporating water from the filtered liquid in the second sample to condense and collect the precipitate. It was expected that the first and the second samples would be the same and the third sample would be pure KNO₃. The results of the x-ray diffraction analysis indicated that the precipitate leaving the cell had a resemblance (according to the database) to several molecules including barium uranium oxide (BaU_{6.24}O_{19.7}), Compreignacite (K₂U₇O₂₂!xH₂O), potassium uranium oxide hydrate (K₂U₇O₂₂!xH₂O), and Schoepite (UO₃!2H₂O). Since there is no Ba in the solution, barium uranium oxide can be discarded. Compreignacite, potassium uranium oxide hydrate, and Schoepite all are possible matches for the unknown precipitate due to their chemical makeup. The most obvious match being Compreignacite due to its ionic state being U⁺⁵ which is believed to be generated from the reduction of U⁺⁶ acquired through this electrochemical technique. The solution precipitated with KOH and the evaporated solution contained a resemblance to only Boltwoodite (K(H₃O)(UO₂)(SiO₄)) therefore this test proved inconclusive for the other two unknowns due to the presence of Si in the identified solution.

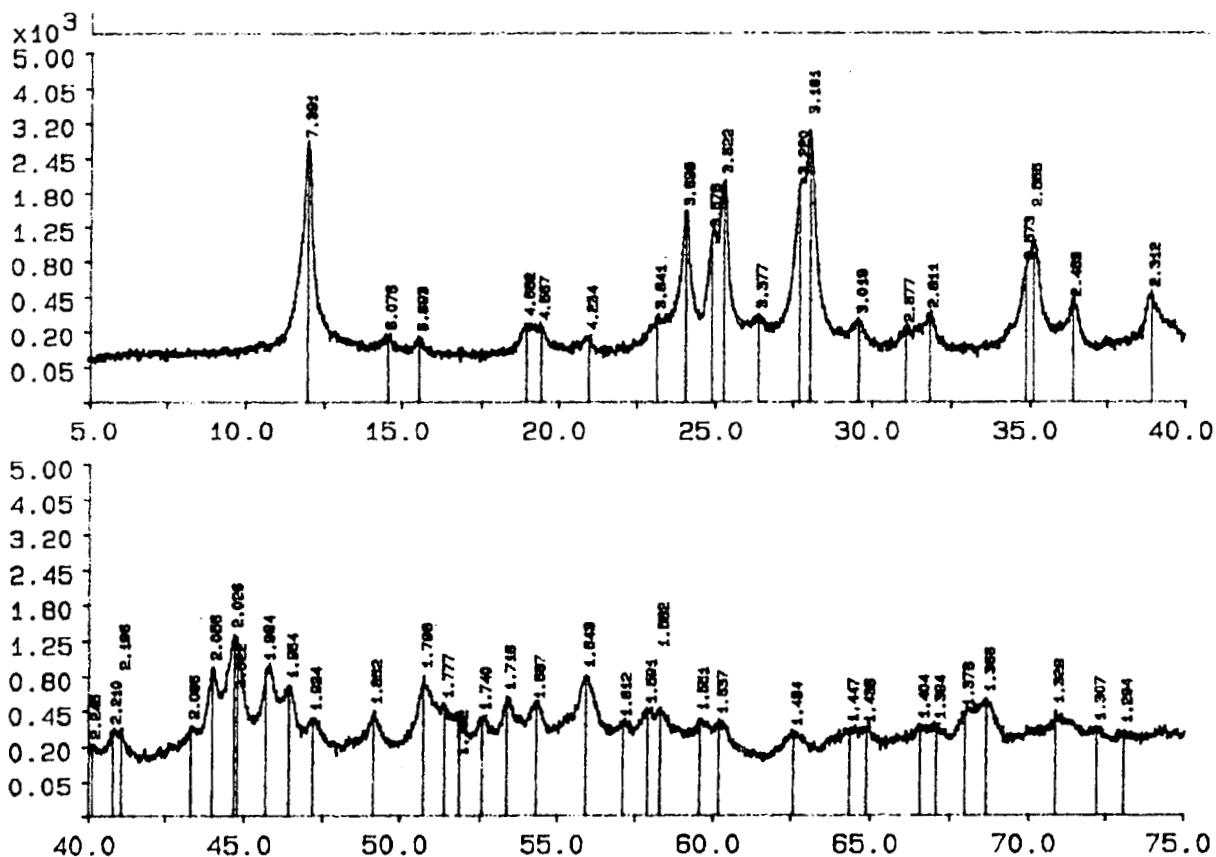


Figure 18. The x-ray diffraction spectrum is similar to $M(\text{UO}_2)_6\text{O}_4(\text{OH})_6 \cdot 8 \text{H}_2\text{O}$, where M may be a +2 valance ion such as barium. Perhaps a +2 uranyl ion may substitute for M in this case.

4.5 Proposed Mechanism

The results are very positive for all types of nanofiber electrodes tested. Several different hypotheses were considered for the mechanism by which uranium is deposited. Xu, who had considered explanations for the effect in his dissertation, pointed out several problems which must be dealt with.¹

- a. The amount of uranium removed from solution is too high to be a simple monolayer of adsorbate. The surface area of the nanofibers is too small by a factor of 10^2 .
- b. The reaction requires carbon nanofibers and is not observed on carbon black or other electrodes. Thus simple electrodeposition does not explain the data.
- c. The reaction requires a bias of -0.9 V . Thus it is not a simple chemical reaction or sorption reaction involving carbon.

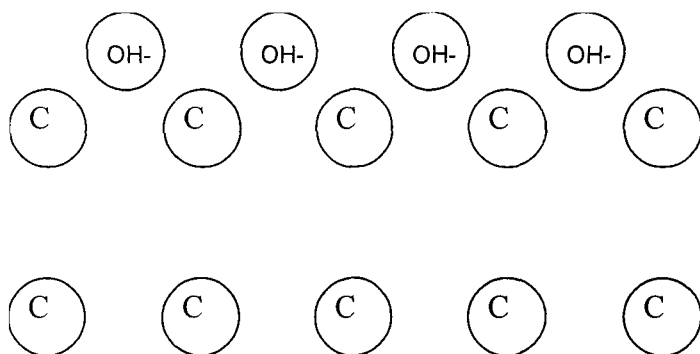
d. The effectiveness of the technique (i.e., the very low concentration values which can be attained) suggests that this can not be a precipitation reaction caused by changing the local pH. In addition, the cell as a whole at WVU becomes more acidic as it operates, whereas the cell at ASI becomes more basic.

Xu had correctly observed that electrosorption as a result of double-layer charging of the carbon electrode can be a viable mechanism for removing uranyl ions from solution. As illustrated below, double layer formation is a consequence of electrostatic attraction between the uranyl ions and the negatively charged carbon edge planes.

Xu had rejected this hypothesis on the basis that the double layer effect would limit the amount of absorption to a monolayer of uranium ions on the surface of the nanofibers. However, Xu had failed to observe that the double layer effect is well known to promote crystal growth in aqueous solutions. Thus the double layer effect can easily result in 10^2 to 10^3 layers of metal oxide deposition, which is observed in the data.

Empirically, this interpretation is attractive because the parameters required for good uranium electrosorption are similar to the parameters required for good behavior in double-layer ultracapacitors. Carbon nanofibers are much more effective than carbon black because of the presence of edge plane sites, which permit the formation of the double layer.

A basic description of the double layer phenomena is as follows. As illustrated below, initially electrostatic charges cause the +2 uranyl atoms to be attracted to the negatively charged cathode. One way to form a double charge layer would be for hydrogen from water to be absorbed on the negative surface leaving a free hydroxyl ion near the surface. This high local hydroxyl concentration can then result in precipitation of uranyl hydroxide solid at the surface.



Conceptual drawing of the formation of a double charge layer at the solid-liquid interface (e.g., with uranyl ions).

4.6 Larger Cell Trials

4.6.1 The 2 Inch Diameter Cell

Both a 2 inch and a 4 inch diameter cell were built and evaluated in this program. The design of these cells is shown in Figure 19. Initial experimentation with these cells

showed that the carbon nanofiber for the working electrode could not be utilized in the loose fiber form that was used in the 1 cm diameter cell. Loose fibers were observed which impacted the electrical continuity of the electrode and hence the operation of the cell. After some experimentation it was found that if the carbon nanofibers were prepared in the form of a mat or paper the electrical continuity of the cell was maintained. Two types of paper were utilized for the experimentation with these cells. The preparation of these papers is given in the experimental section. Both contain a small amount of binder which produces a form wherein the carbon nanofibers are confined. One uses PAN based carbon fibers as the binder and the other uses a rubber latex as the binder. The one using the rubber latex binder was preferred since it appeared to provide better integrity.

Seventeen samples from experiments using the 2 inch cell were analyzed using the DPV technique. Each sample from the 2 inch diameter cell was analyzed at least two times and the average of the values was reported as the concentration in ppm of U in the sample. The collected data are summarized in Table 6.

Unfortunately the pH of the solution used for this set of experiments was incorrect. The initial value was 2.2 rather than 3.5. Consequently the only way to compare the data with previous data and determine the efficacy of the cell is to compare this cell data with the values generated at a pH of 2, i.e. Figure 15. This comparison suggests that for the majority of these samples this larger cell worked as efficiently as the small cell.

Table 6. Performance of 2" diameter cell.

Sample Number	U Conc (ppm)	pH	Fiber Used	Sampling Time, min
100 ppm U control	77.9	2.18		
042502-01	30.4	--	PR-24-AG/latex ^A	34
042602-01	30.2	--	PR-24-AG/latex	23
050102-01	2.1	--	PR-24-AG/latex	3
050102-02	6.8	--	PR-24-AG/latex	10
050102-03	0.9	--	PR-24-AG/latex	39
050102-04	<0.5	--	PR-24-AG/latex	76
051502-01	30.6	2.81	PR-19-AG/paper ^B	97
052102-01	<0.5	2.44	PR-19-AG/paper	48
052902-01	8.0	2.60	PR-19-AG/paper	70
-053002-01	3.7	2.60	PR-19-AG/paper	64
053002-02	57.8	2.44	PR-19-AG/paper	53
060302-01	60.8	2.40	PR-19-AG/paper	58
060302-02	7.9	2.44	PR-19-AG/paper	54
060402-01	28.0	1.30	PR-19-AG/paper	47
060502-02	33.8	1.94	PR-19-AG/paper	72
061702-01	33.1	1.47	PR-19-AG/paper	228

Some pH values not collected due to broken pH electrode or lack of solution

A = paper prepared from PR-24-AG containing 5 wt% rubber latex

B = paper prepared from PR-19-AG, PAN carbon fibers and a binder.

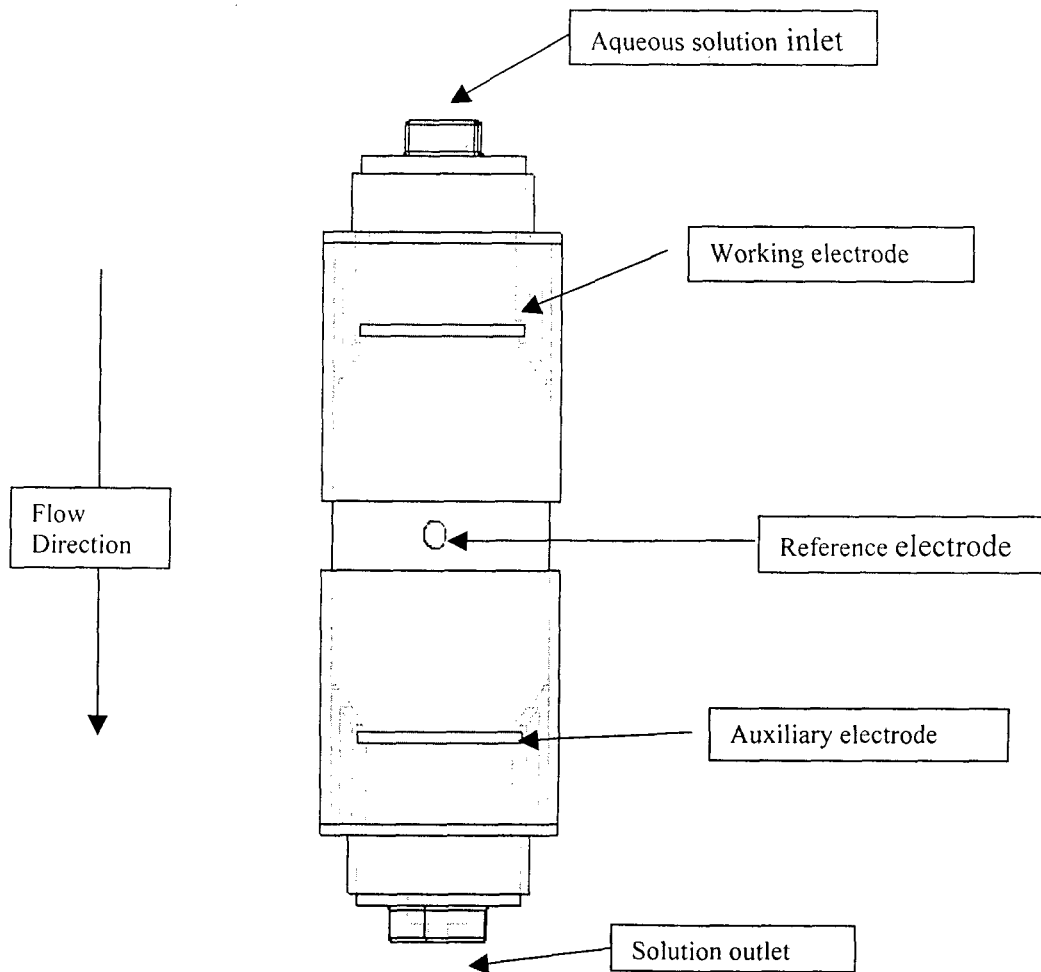


Figure 19. Schematic of Large Electrolytic Cell

4.6.2 The 4 Inch Diameter Cell

The performance of the largest cell (4 inch diameter) was evaluated by pumping a fixed volume (4.75 L) of a 1000 ppm solution of uranyl nitrate in 0.1 molar KNO_3 (pH 3.5) continuously through the cell. The cell volume was 170 ml and the pumping rate was 1.17 L/min. Samples taken at fixed intervals as shown in Table 7 were analyzed at WVU. Due to a problem with noise in the analytical system uranium levels below 5 ppm could not be determined. However all the samples taken had uranium concentrations below 5 ppm. This shows a very effective removal process is operating. The particular fiber used also appeared to be effective when used in the 2" diameter cell.

Table 7. Performance of 4" diameter cell.

Sample Number	U Conc (ppm)	Sampling Time, min
Large cell run 2-1, initial	1000	0
Large cell run 2-2	<5	8
Large cell run 2-3	<5	18
Large cell run 2-4	<5	22
Large cell run 2-5	<5	31
Large cell run 2-6	<5	57
Large cell run 2-7	<5	77
Large cell run 2-8	<5	158

The fiber used was PR-24-AG/latex and the initial pH was 3.5.

V. CONCLUSIONS AND RECOMMENDATIONS

The purpose of this study was to investigate the effects of nanofibers properties on the performance of uranium removal with respect to their total adsorption capacity. In addition, the results of Stover's variation of experimental parameters of pH, adsorption/desorption cycling, and applied potential were revisited and verified. Finally, the optimum regeneration sequence was found for the most effective use of the carbon electrode.

It was found that for a 1 cm diameter cell using an inlet flow rate of 0.7 ml/min and inlet concentration of 100 ppm, the total absorptive capacity of PR-21 PS and PR-18 post ox was much greater than the other three nanofibers tested. Uranium mass adsorption ratios m_u/m_c equal to 0.621 and 0.523 respectively were observed. This is considerably higher than similar measurements for PR-19-HT electrodes, which achieved a uranium mass adsorption ratio of 0.373. These results are considerably lower than those of Stover who reported a uranium mass ratio 5.45.

Three comparison trials achieved virtually identical results with PR-18-post-ox nanofibers. The results for recreating the pH, adsorption/desorption, and applied potential were nearly identical for Stover's and the present experiments. From the evidence demonstrated above, it can be concluded that the pH needs to be between 3 and 5, the potential must be at least -0.5 V, and it is possible to have multiple loading / stripping runs on the same carbon without loss of performance.

Perhaps the most interesting discovery was a method by which nearly total regeneration of the carbon can be achieved. It was found that the pH of 2.0 with an applied potential of +1.0 V (dc) achieved 70% removal efficiency in only 60 min. By contrast, with a pH of 3.5 at +1.0 V (dc) potential for 100 min, the removal efficiency was only 44%. For the latter case, a small quantity (~1 weight percent) of solid precipitate was collected. With a pH of 2.0 in which the uranium precipitate was completely dissolved.

The ability of carbon nanofibers to absorb uranium from aqueous solution was further demonstrated using both a 2 inch and a 4 inch diameter cell. For these cells the carbon nanofiber based electrodes that operated satisfactorily were those based on a paper or mat form of the carbon nanofibers, probably due to the retention of electrical continuity during operation.

From the results in this study, it has been demonstrated that the use of carbon nanofibers as an electrode for uranium removal is a viable water treatment option.

VI. REFERENCES

1. Xu, Y., "Electrochemical Treatment of Metal-bearing Aqueous Wastes Based on Novel Forms of Carbon", Ph.D. Dissertation, Dept. of Chemical Engg., West Virginia University, 1999.
2. Stover, S., "Removal of Uranium from Aqueous Wastes using Electrically Charged Carbon Nanofibers", M.S. Dissertation, Dept. of Chemical Engg., West Virginia University, 1999.
3. Akimov, G.V. and I.L. Rosenfeld, In: *Issledovaniya v oblasti elektrokhimicheskogo i korrozionnogo povedeniya metallov i splavov*, Moscow, Oborongiz, 1950.
4. Udal'tsova N.I., *Chemico-Analytical Properties of Uranium and Its Compounds in Analytical Chemistry of Uranium*, Ed. P.N.Palei, Ann Arbor, London, GB, 1970.
5. Seaborg, G.T and J. Katz, *The Actinide Elements*, New York, McGraw-Hill, 1954. See also Katz, J. and E. Rabinowitch. *The Chemistry of Uranium*, Nila, Wiley, 1951.
6. Xu, op cit.
7. Ibid.
8. Pourbaix, M., *Atlas of Electrochemical Equilibria in Aqueous Solutions*, Pergamon Press, New York, 1966.
9. Ibid.
10. Stover, op cit.
11. Ibid.
12. Ibid.